A 28-GHz Massive MIMO Receiver Deploying One-bit Direct Detection with Wireless Synchronization

Hang Zhao, Michael Green
Department of Electrical Engineering and Computer Science
University of California Irvine, CA, 92697-2625
Email: {hangz8,mgreen}@uci.edu

***Abstract*—A 28-GHz one-bit direct-detection based MIMO receiver with wireless LO distribution is presented. Unlike a conventional MIMO structure, in this work the antenna receives both RF and the broadcast single-ended LO, and directly converts them to an IF signal by using a simple low-power square-law detector without the need for a conventional mixer or LO buffers. An LNA with a notch filter is designed to help reduce the non-idealities that appear when the input LO power is lower than that of the RF. A 1-GS/s symbol rate with a high error-vector magnitude is achieved with a power consumption of 33 mW by using a 0.18um SiGe BiCMOS process.**

***Index Terms*—28-GHz, MIMO receiver, additive mixing, wireless distributed LO, notch filter, quadrature demodulation.**

I. Introduction

The deployment of large arrays of antennas for wireless communications, known as massive MIMO, is seen as a critical technology for achieving major advancements in spectral efficiency needed to meet the ever-increasing demand for wireless services [1]. A separate RF chain implemented behind each antenna can maintain full baseband beamforming flexibility for a massive MIMO system but at the expense of high power dissipation. An analog RF front-end using phase shifters or hybrid structures can reduce the power consumption but will compromise the beamforming flexibility. This work focuses on maintaining a separate receiver chain for each antenna, while reducing the cost and power for each individual chain by deploying direct detection. In this approach the IF is recovered directly from the received broadcast LO and RF by additive mixing.

Section II describes the theory and operation of the direct-detection based receiver. Sections III and IV describe in detail the circuit design and give simulation results. Conclusions are given in Section V.

II. Technical Approach

A. Direct Detection Receiver - Theory and System

As an alternative to multiplier-based mixing, direct detection is based on additive mixing. As illustrated in Fig. 1, the envelope of the composite LO and RF signal contains the desired IF signal; this envelope can be extracted by a simple square-law detector. To illustrate this process, the demodulation of a BPSK-modulated signal is first considered. This signal (ignoring the channel losses) can be expressed as:

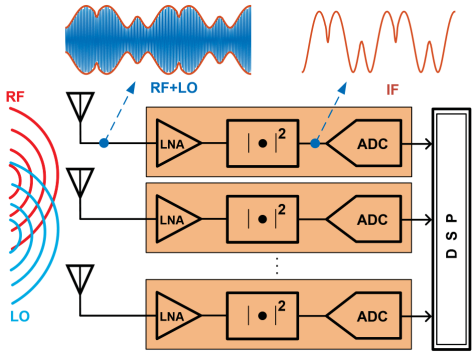

Fig. 1. MIMO receiver array deploying direct detection.

$$V_{in} = V_{RF}(t) \cdot \cos(\omega_{CR} t) + V_{LO} \cdot \cos(\omega_{LO} t) \quad (1)$$

where $V_{RF}(t) \equiv K(t) \cdot V_{BB}$; V_{BB}, V_{LO}, and $|V_{RF}(t)|$ are the amplitudes of the baseband, received LO and RF signals, respectively; ω_{CR} and ω_{LO} are the carrier and LO frequencies, respectively; $K(t) \in [-k, +k]$, and k is a constant that depends on the transmitter gain.

The envelope of the composite signal, $\mathrm{env}(V_{in})$, is given by:

$$\sqrt{V_{RF}^2(t) + V_{LO}^2 + 2V_{LO}V_{RF}(t) \cdot \cos\left[(\omega_{CR} - \omega_{LO})\, t\right]} \quad (2)$$

where the third term under the square-root is the IF signal. By using a square-law detector, such as a diode [2] or a single-gate mixer [3] with proper filtering, the IF can be recovered without the distortion caused by the square-root, then digitized by the ADC and applied to the DSP.

B. Wireless Synchronization

The primary benefit of a direct-detection based receiver is that it only requires a single-ended LO, which can be easily provided wirelessly. The wireless synchronization system [4] entails the deployment of a "dummy" radiating antenna placed a short distance away from the intended MIMO antenna array,

978-1-7281-3320-1/20/$31.00 ©2020 IEEE

which broadcasts the LO signal for demodulation. The LO power attenuation follows the inverse square law of free-space propagation with respect to the MIMO array's dimension, while wired implementations suffer from an exponential attenuation with respect to the trace length due to the skin effect.

Conventional quadrature demodulation systems require a quadrature LO for separating the I/Q signals. However, for the direct detection receiver, since the broadcast LO and RF bands are very close, separating out the pure LO from the composite signal for the quadrature phase generation is difficult. Instead, digital quadrature demodulation is applied in the proposed receiver system, where the recovered IF signal is applied directly to an ADC with sampling rate $f_s = 4f_{IF}$. In this way, all the I/Q components will be digitized and can be separated within DSP. Subsampling [5] can also be used if the IF frequency is higher than the baseband to avoid operating the ADC in a high sampling-rate. An added benefit is that buffers and other blocks needed for generating quadrature LO used in a conventional receiver chain are no longer needed, leading to reductions in power and complexity of the system.

C. LO Power Requirements for Proper Downconversion

In some applications, due to strict regulatory restrictions on radiated power, the LO power has to be very low. This power can be boosted to provide enough conversion gain at the mixer by increasing the LNA gain. However, when the input LO power is smaller than the RF power, the appearance of glitches, illustrated in Fig. 2(a), will occur in the recovered IF signal at each signal's phase reversing region, degrading the IF's SNR. On the other hand, as shown in Fig. 2(b), the glitches becomes less pronounced when the LO power is larger than that of the RF. The following modeling explains the reason:

Assuming the detector's conversion gain is unity, after the composite input signal (1) is fed to a square-law detector, the detected output with high-frequency components filtered is given by:

$$V_{out} = \frac{1}{2}{V_{RF}}^2(t) + \frac{1}{2}{V_{LO}}^2 + V_{LO}V_{RF}(t)\cdot\cos\left[(\omega_{CR}-\omega_{LO})t\right] \tag{3}$$

For an ideal unshaped BPSK baseband signal with instantaneous phase changes, its baseband and RF amplitudes V_{BB} and $|V_{RF}(t)|$, respectively, are constant. Thus the first two terms in (3) only introduce a dc term to V_{out}, which can be easily filtered out. However, in the more realistic case where the phase inversion is not instantaneous during each transition, the value of ${V_{RF}}^2(t)$ will momentarily decrease toward zero and then return back, resulting in a glitch in the recovered IF signal. When the LO is at least 10 dB higher than the RF, the glitches' influence on the IF becomes much smaller and can be ignored, as illustrated in Fig. 2(b). In order to achieve this condition, either the LO power can be boosted or the RF power can be reduced prior to the mixer. In this work, a low-Q notch filter is used to reduce the RF power, which will be discussed in the next section.

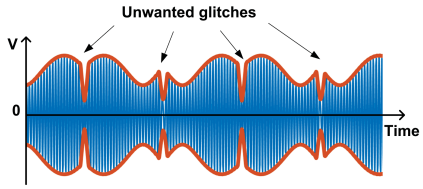

(a)

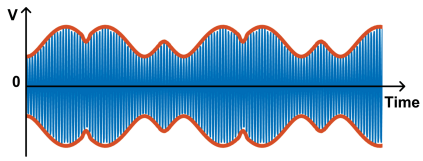

(b)

Fig. 2. The envelopes of added LO and RF with different power levels: (a) when $P_{LO}/P_{RF} = -10$ dB, glitches appear at the phase reversing region; (b) when $P_{LO}/P_{RF} = 10$ dB, the glitches are largely reduced and can be ignored.

III. Circuit Design

A. System Architecture and Implementation

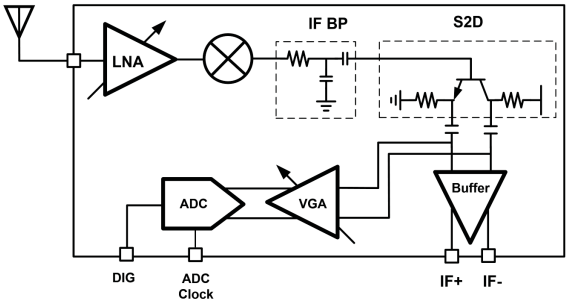

(a)

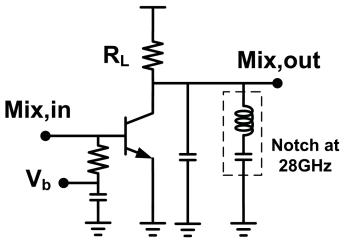

(b)

Fig. 3. (a) Receiver-chain architecture; (b) single-gate mixer with notch filter.

A block diagram of one receiver chain is shown in Fig. 3(a). A three-stage LNA that includes notch filters is used to reduce the RF power in order to suppress the glitches. A square-law detector is implemented using a single-gate BJT mixer as shown in Fig. 3(b). The output current of the BJT, which is an exponential function of $V_{mix,in}$, can be represented by the following Taylor series:

$$I_C \approx I_{CQ}\left[1 + \frac{V_{mix,in}}{V_T} + \frac{1}{2}\left(\frac{V_{mix,in}}{V_T}\right)^2 + \ldots\right] \tag{4}$$

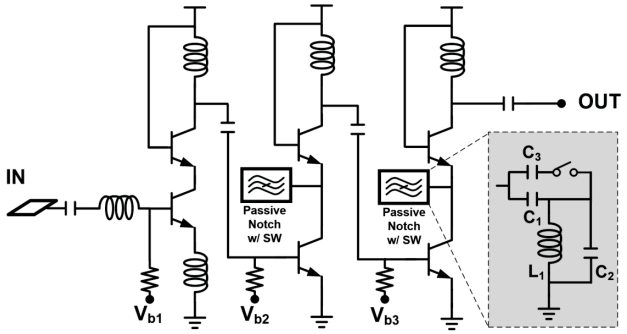

(a)

Fig. 4. Three-stage LNA with switchable notch filters. When the switches is open, two notch filters can provide up to 10dB gain difference between the LO and RF band.

where V_B and V_T are the dc bias and the thermal voltage, respectively, and I_{CQ} is the quiescent current. The frequency components of third and higher-order harmonics will be filtered out by the mixer's capacitive load together with the following IF bandpass filter. The fundamental frequency is filtered out by the 28-GHz notch filter at the load. After the filtering provided by the IF bandpass filter shown in Fig. 3(a), the second harmonic in (4) provides the amplified IF signals. Together with (3), the conversion gain is expressed as:

$$A_{conv} = \frac{IF(V_{mix,out})}{V_{RF}(t)} = I_{CQ} R_L \frac{V_{LO}}{2{V_T}^2} \tag{5}$$

If the provided LO power is larger, the power consumption of the mixer can be reduced to achieve a given conversion gain. The signal feed-through noise can be largely filtered by the IF-bandpass filter shown in Fig. 3(a). Then the recovered single-ended IF will be converted to differential and fed to the VGA, which can provide extra gain for the IF signal. The power consumption of each receiver chain is further reduced by using a simple one-bit ADC, which is sufficient for QPSK modulation. Although high-order modulation schemes exist, the lower power consumption for each individual chain enables a larger array of antennas with a fixed power budget. In this way a higher overall spectral efficiency can be achieved as discussed in [4]. The one-bit ADC is implemented on-chip as a comparator.

B. Three-Stage LNA with Switch-Controlled Notch Filter

In order to suppress the glitches and increase the RF input power range, an LNA is implemented with a set of switched notch filters, shown in Fig. 4. When the switches are open, the notch filter together with the LNA can provide up to 10 dB gain suppression at the RF center frequency while maintaining a flat gain over the RF band.

The passive notch filter can provide a low impedance at unwanted frequencies, corresponding to the RF band, while keeping a high impedance at the desired frequency, corresponding to the LO frequency. As discussed in [6] the inductor and capacitor values can be determined by the following equations:

$$f_{RF-center} = \frac{1}{2\pi\sqrt{L_1 \cdot (C_1 + C_2)}} \tag{6}$$

$$f_{LO} = \frac{1}{2\pi\sqrt{L_1 \cdot C_1}} \tag{7}$$

The gain difference between the unwanted and desired bands is limited by both the Q of inductor L_1 and the frequency difference between these two bands. A simple third-order passive filter structure is used in this work. To further increase the gain difference, two identical filters are used at both the second and third stage of the LNA. The gain variation over the RF band is less than 2 dB while the gain difference between the RF and LO can be up to 10 dB for 2-GHz IF. The first stage of the LNA is implemented as a conventional structure in order to obtain good input matching. Since each low-Q notch filter introduces only a small amount of noise that will be suppressed by the first-stage LNA, the NF of the LNA is low over the band of interest.

For the case where the input LO power is already higher than that of the RF, the use of a notch filter is no longer necessary. In this case the switches can be closed to connect capacitor C_3, together with the finite on-resistance of the switch, in parallel with C_1. The larger effective capacitance will shift the notch to a much lower frequency with lower Q. As a result, the frequency response within the RF band becomes similar to that of a normal multi-stage LNA.

IV. Simulation Results

Using the TowerJazz sbc18 BiCMOS process design kit, a simulation of the complete post-extraction layout was performed for the individual receiver chain including the pads, ESD, and flip-chip bumpers; this simulation includes transient noise for all components together with the LO and carrier's phase noise. Fig. 5 shows the LNA simulation results corresponding to both states of the switched notch filter. The LNA exhibits low reflection (S11 $\leq$ –15 dB) over 26-30 GHz. When the notch filter switch is open, the noise figure (NF) of the receiver is 4.26 dB in the RF band, and 4.14 dB in the LO band. When the switch is closed, the NF is around 4.1 dB over 26-30 GHz. When the switch is open, the LNA provides 8 dB gain suppression in the RF band while providing less than 2 dB gain variation within the channel bandwidth of 500 MHz. Fig. 6 shows the power spectrum density (PSD) of the input and output signals of the LNA with the notch filter. The power difference between LO and RF is boosted by around 8 dB at the output.

When the switch is closed, the LNA performs as a normal amplifier, and can support larger channel bandwidth with lower IF frequency. Fig. 7(a) shows the error vector magnitude (EVM) vs input power for three different LO power levels with 1-GS/s QPSK modulation. The EVM is limited by the noise when the RF power is higher than the LO, and limited by distortion and glitches when RF power is lower than the LO. The peak EVM is achieved when the RF and LO power are nearly the same. Fig.7(b) shows the constellation diagram

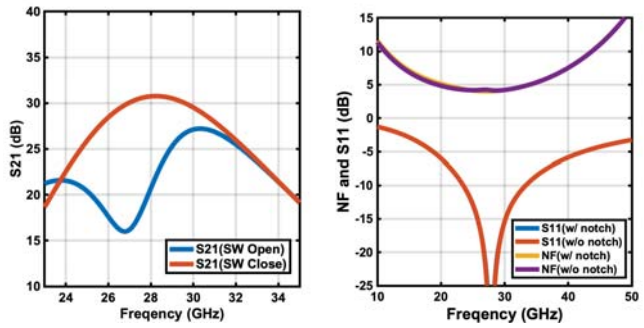

(a) (b)

Fig. 5. (a) LNA gains for both switch states. When the switches are open, the notch filter suppresses the gain at RF band (27GHz) for around 8dB compared with the LO (29GHz); (b) NF and S11 for both switch states.

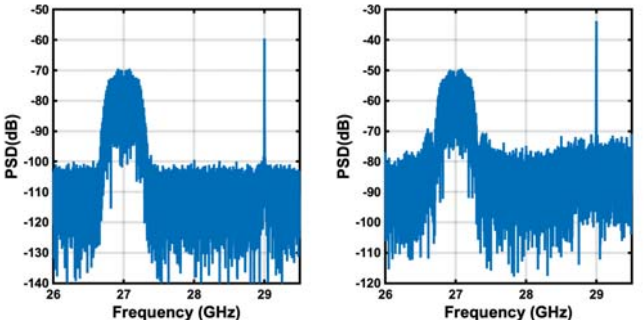

(a) (b)

Fig. 6. (a) LNA input spectrum; (b) LNA output spectrum.

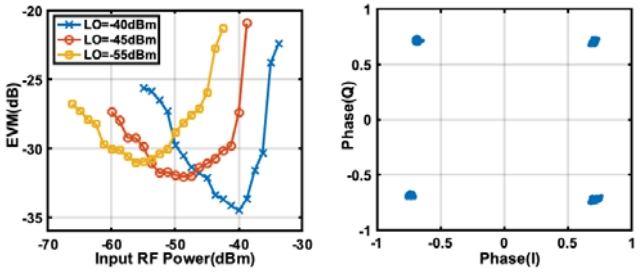

(a) (b)

Fig. 7. (a) EVM vs. RF input power; (b) constellation diagram with RF/LO power -50/-45 dBm, achieving -32dB EVM.

corresponding to a -50 dBm, 27 GHz RF center frequency and a -45 dBm, 28 GHz LO, with a symbol rate of 1 GS/s. Using a supply voltage of 1.6V, the power consumption of LNA and mixer are 20.8 mW and 3 mW, respectively. The converter together with the VGA and one-bit ADC (1.8V supply) consumes 4.2 mW. The digital I/O buffers consume 5 mW. A 33 mW total power consumption is achieved not including the IF band output buffers used for testing. Table I compares the main parameters of the receiver chain with other works [7]-[9].

TABLE I
PERFORMANCE COMPARISON WITH OTHER 28-GHz RECEIVERS

Comparison Table	This work	[7]	[8]	[9]
Process	0.18 SiGe	0.18 SiGe	65nm	28nm
Freq. (GHz)	28	28	28	28
NF (dB)	4.2	4.6	4.1	4.4
Symbol Rate, Max (GS/s)	1	1.5	2.5	0.4
Data Rate, Max (Gb/s)	2	6	15	2.4
Supply Voltage (V)	1.6/1.8	1.2/2.2	-	1/1.8
RX Power/el. (mW)	33*	130	148	42
Chip Area/el. (mm^2)	0.94**	2.92	3	1.16

*Includes the on-chip ADC. **Receiver only.

V. Conclusion

A 28-GHz MIMO receiver chain deploying one-bit direct detection for full beamforming flexibility has been described. Low power consumption for each individual chain is achieved by using the additive-mixing based structure together with the wireless LO synchronization. A low-power one-bit ADC is also implemented on-chip to enable more chains implemented for MIMO array with the same power budget. The design also considers the LO's radiated-power strictly restricted system. The non-idealities appear when input LO's power is smaller than the RF can be reduced by the three-stage LNA with the notch filters. The symbol-rate of 1 GS/s has been achieved with the total power consumption of 33 mW.

References

[1] L. Lu, G. Li, A. Swindlehurst, A. Ashikhmin and R. Zhang, "An overview of massive MIMO: Benefits and challenges," *IEEE J. of Sel. Topics in Signal Processing*, vol. 8, no. 5, pp. 742–758, Oct. 2014.

[2] D. Roddy, *Radio and Line Transmission: The Commonwealth and International Library: Electrical Engineering Division,* Vol. 2. Elsevier, 2013.

[3] S. Emami, *et al.*,"A 60-GHz down-converting CMOS single-gate mixer," in *2005 IEEE Radio Frequency integrated Circuits (RFIC) Symposium - Digest of Papers,* Long Beach, CA, pp. 163-166.

[4] A. Mezghani and A. L. Swindlehurst,"mmWave massive MIMO with simple RF and appropriate DSP." in *2017 51st Asilomar Conference on Signals, Systems, and Computers,* Pacific Grove, CA, pp. 277-284.

[5] K.-P. Pun, *et al.*,"Quadrature sampling schemes with improved image rejection" *IEEE Transactions on Circuits and Systems II: Analog and Digital Signal Processing,* vol. 50, Sept. 2003, pp. 641-648.

[6] T.-K. Nguyen, *et al.*, "Image-rejection CMOS low-noise amplifier design optimization techniques," *IEEE Transactions on Microwave Theory and Techniques,* vol. 53, Feb. 2005, pp. 538-547.

[7] K. Kibaroglu, M. Sayginer, and G. M. Rebeiz, "A Low-Cost Scalable 32-Element 28-GHz Phased Array Transceiver for 5G Communication Links Based on a 2×2 Beamformer Flip-Chip Unit Cell," *IEEE Journal of Solid-State Circuits,* vol. 53, May 2018, pp. 1260-1274.

[8] J. Pang, *et al.*, "A 28-GHz CMOS Phased-Array Transceiver Based on LO Phase-Shifting Architecture With Gain Invariant Phase Tuning for 5G New Radio." *IEEE Journal of Solid-State Circuits,* vol. 54, May 2019, pp. 1228-1242.

[9] J.D. Dunworth *et al.*, "A 28GHz Bulk-CMOS dual-polarization phased-array transceiver with 24 channels for 5G user and basestation equipment." in *2018 IEEE International Solid-State Circuits Conference-(ISSCC),* San Francisco, CA, pp. 70-71.